

Domain wall solutions with Abelian gauge fields

J.S. Rozowsky

Physics Department, Syracuse University, Syracuse, NY 13244-1130, U.S.A.
rozowsky@phy.syr.edu

R.R. Volkas

*School of Physics, Research Centre for High Energy Physics, The University of Melbourne,
Victoria 3010, Australia.*
r.volkas@physics.unimelb.edu.au

K.C. Wali

Physics Department, Syracuse University, Syracuse, NY 13244-1130, U.S.A.
wali@phy.syr.edu

ABSTRACT: We study kink (domain wall) solutions in a model consisting of two complex scalar fields coupled to two independent Abelian gauge fields in a Lagrangian that has $U(1) \times U(1)$ gauge plus \mathbb{Z}_2 discrete symmetry. We find consistent solutions such that while the $U(1)$ symmetries of the fields are preserved while in their respective vacua, they are broken on the domain wall. The gauge field solutions show that the domain wall is sandwiched between domains with constant magnetic fields.

Contents

1. Introduction	1
2. The Model	2
3. Numerical Solutions	6
4. Discussion	10
5. Conclusions	11

1. Introduction

Over the last thirty years or so, the study of solitonic solutions to classical field theories has yielded many interesting results of wide relevance to particle physics, cosmology and condensed matter physics. The more recent fascination with brane-world models of particle physics and cosmology has added new motivation for these kinds of investigations. In this paper we will study a simple model of two complex scalar or Higgs fields ϕ_1 and ϕ_2 coupling to two different $U(1)$ gauge fields $A_{1\mu}$ and $A_{2\mu}$, with the added feature of an exact discrete \mathbb{Z}_2 symmetry under the interchange $1 \leftrightarrow 2$. We will derive solutions to the coupled classical field equations that exhibit a kink or domain wall form for the scalar fields. The nature of the gauge field configurations self-consistently coupled to the Higgs kinks will be our primary object of study. A similar model, without the discrete exchange symmetry was studied some-time ago by Witten [1] in the context of a superconducting string solution. The model was investigated in more detail by MacKenzie [2] to show that while a symmetry is preserved in the vacuum, unexpected topological structures can arise in the interior of a domain wall. More recently, Lempriere and Shellard [3] have reported on the behavior and stability of the superconducting currents in Witten’s model.

Our own motivation for this rather abstract investigation lies with the symmetry breaking mechanism proposed in Ref. [4] in the context of brane world models and dubbed as the “clash of symmetries”. Briefly, Ref. [4] examines a toy model with Higgs fields in three triplet representations of a *global* $SU(3)$ symmetry, where a discrete permutation symmetry between the triplets is enforced. Omitting inessential complications, the vacuum states of the theory spontaneously break $SU(3)$ down to $SU(2)$, as well as spontaneously breaking the discrete

symmetry. Kink solutions are derived that interpolate between vacua invariant under *differently embedded* $SU(2)$ subgroups.¹ For instance, one can have I -spin asymptotically preserved on one side of a domain wall, with V -spin on the other. Although the unbroken subgroups on both sides are isomorphic, the different embeddings within the parent group cause additional symmetry breakdown at all non-asymptotic points. This additional symmetry breaking is the “clash”. The idea is that some of the symmetry breaking we see in our universe might be due to such a clash, if our world is indeed a brane in a higher dimensional space.

This idea is still at the developmental stage; no realistic brane-world model building using the clash mechanism has yet been attempted, to our knowledge, though Ref. [6] reports on some recent progress. In the course of thinking about the clash of symmetries idea, however, an even simpler model field theory with $U(1)$ factors and interchange symmetries between the different sectors naturally presented itself as a useful theoretical laboratory. The model studied in this paper arose in exactly this way, though, of course, it is also entitled to an independent existence as a simple-but-not-too-simple vehicle for the study of gauge fields coupled to domain wall Higgs configurations. From this perspective, our work is relevant to general studies of superconducting topological solitons, as in Refs. [1–3, 7, 8] for example. From the clash of symmetries perspective, the present exercise begins the study of the breakdown of *local* continuous symmetries.

The rest of this paper is structured as follows: In Sec. 2, the model and the field equations are presented. The numerical study of kink solutions to these equations is then presented in Sec. 3, while Sec. 4 provides a physical explanation for the solutions. Section 5 contains some concluding remarks.

2. The Model

Using the the notation of [4] we start with the action for two complex scalar fields $\phi_{1,2}$ coupled to different $U(1)$ gauge fields $A_{1,2}$. To the overall $U(1) \times U(1)$ gauge symmetry we add a \mathbb{Z}_2 discrete symmetry which interchanges the scalars, $\phi_1 \leftrightarrow \phi_2$ and the gauge fields, $A_1 \leftrightarrow A_2$. The discrete symmetry makes the two gauge coupling constants equal in magnitude. The Lagrangian is

$$\mathcal{L} = -\frac{1}{4}F_1^{\mu\nu}F_{1\mu\nu} - \frac{1}{4}F_2^{\mu\nu}F_{2\mu\nu} + (D_1^\mu\phi_1)^*(D_{1\mu}\phi_1) + (D_2^\mu\phi_2)^*(D_{2\mu}\phi_2) - V(\phi_1, \phi_2), \quad (2.1)$$

where

$$V(\phi_1, \phi_2) = \lambda_1 (\phi_1^*\phi_1 + \phi_2^*\phi_2 - v^2)^2 + \lambda_2\phi_1^*\phi_1\phi_2^*\phi_2. \quad (2.2)$$

The covariant derivatives in the Lagrangian are given by

$$D_{1\mu} = \partial_\mu - ieA_{1\mu} \quad , \quad D_{2\mu} = \partial_\mu - ieA_{2\mu}. \quad (2.3)$$

¹Qualitatively similar solutions, but to a different theory with a different motivation were discovered by Pogosian and Vachaspati in Ref. [5].

The Higgs potential admits two vacuum solutions:

$$\text{Vacuum 1 : } \langle \phi_1^* \phi_1 \rangle = v^2 \quad \langle \phi_2^* \phi_2 \rangle = 0, \quad (2.4)$$

$$\text{Vacuum 2 : } \langle \phi_1^* \phi_1 \rangle = 0 \quad \langle \phi_2^* \phi_2 \rangle = v^2. \quad (2.5)$$

These two vacua are degenerate and are the global minima of the potential for the parameter regime

$$\lambda_1 \geq 0 \quad \text{and} \quad \lambda_2 \geq 0. \quad (2.6)$$

We would like to construct domain wall solutions by requiring the scalar Higgs fields to asymptote to different respective vacua on either side of the wall. We will be interested in the behavior of the corresponding gauge fields for this kind of Higgs configuration. The boundary conditions for the scalars are

$$|\phi_1(z)| = \begin{cases} 0 & z \rightarrow -\infty \\ v & z \rightarrow \infty \end{cases} \quad \text{and} \quad |\phi_2(z)| = \begin{cases} v & z \rightarrow -\infty \\ 0 & z \rightarrow \infty \end{cases}, \quad (2.7)$$

where z is the direction perpendicular to the domain wall.

It is straightforward to compute the equations of motion for the Higgs fields

$$D_{a\mu} D_a^\mu \phi_a = -\frac{\partial V}{\partial \phi_a^*} = -2\lambda_1 \phi_a (\phi_a^* \phi_a + \phi_b^* \phi_b - v^2) - \lambda_2 \phi_a \phi_b^* \phi_b, \quad (2.8)$$

where a, b are either 1, 2 or 2, 1 respectively. The equations of motion for the gauge fields are similarly given by

$$\partial_\mu F_a^{\mu\nu} = 2e \text{Im} [\phi_a^* (\partial^\nu - ieA_a^\nu) \phi_a]. \quad (2.9)$$

Since we are going to be looking for static domain wall solutions (i.e. static 1 + 1 solitons), we search for solutions that depend on z but are independent of all the other spatial coordinates and time t . In order to simplify our equations we make use of the temporal gauge, $A_0 = 0$. With these choices the equations of motion reduce to

$$A_{1z} = \frac{\alpha'_1}{e}, \quad (2.10)$$

$$A''_{1x,y} = 2e^2 A_{1x,y} R_1^2, \quad (2.11)$$

$$R_1'' = e^2 (A_{1x}^2 + A_{1y}^2) R_1 + 2\lambda_1 R_1 (R_1^2 + R_2^2 - v^2) + \lambda_2 R_1 R_2^2, \quad (2.12)$$

where prime denotes a derivative with respect to z and $\phi_a \equiv R_a(z) e^{i\alpha_a(z)}$. The corresponding equations for the fields with subscript 2 can be obtained simply by exchanging subscripts 1 and 2. We see in eqn. 2.10 that the z components of both gauge fields are pure gauge and because neither $A_z(z)$ nor $\alpha(z)$ couple to the physical degrees of the system, they can be neglected.

The coupled differential equations for this system nominally involves six degrees of freedom (one scalar and two gauge degrees of freedom for each field). However, since the x and y

components of each gauge field enter quadratically into their respective Higgs field equations of motion, it is possible to rotate to a new basis \tilde{x} and \tilde{y} where one only needs keep track of one component of each gauge field. Note that the directions perpendicular to z in which each of the gauge fields A_1 and A_2 point are independent. We therefore have only four degrees of freedom to non-trivially solve for.

The equations we would like to solve are then

$$A_1'' = 2e^2 R_1^2 A_1, \quad (2.13)$$

$$R_1'' = e^2 A_1^2 R_1 + 2\lambda_1 R_1 (R_1^2 + R_2^2 - v^2) + \lambda_2 R_1 R_2^2, \quad (2.14)$$

and $1 \leftrightarrow 2$. We have suppressed the spatial subscripts on the gauge fields, A .

For a domain wall solution the scalar fields must obey the boundary conditions in eqn. 2.7. Thus, by analyzing eqn. 2.13 we see that the gauge fields are required to have the following asymptotic behavior:

$$A_1(z \rightarrow \infty) = e^{-\sqrt{2}ev|z|} \rightarrow 0 \quad \text{and} \quad A_2(z \rightarrow -\infty) = e^{-\sqrt{2}ev|z|} \rightarrow 0. \quad (2.15)$$

We observe that this asymptotic behavior is also consistent with eqn. 2.14. The values of $A_1(-\infty)$ and $A_2(\infty)$ are seemingly unconstrained by any of our differential equations. However, note that when $z \ll -1$ for $A_1(z)$ or when $z \gg 1$ for $A_2(z)$ the solutions become linear functions of z , the asymptotic solutions to eqn. 2.13. The linear solutions are due to the requirement that $R_1(z)$ and $R_2(z)$ vanish as $z \rightarrow -\infty, +\infty$ respectively (this is because we require them to be kink solutions). Thus, the only allowed values of $A_1(-\infty)$ and $A_2(\infty)$ are either a *constant* (corresponding to constant asymptotic behaviour) or $\pm\infty$. Consistent with this, we will also impose the boundary conditions

$$A_1'(z = -\infty) = \text{const.} \neq 0 \quad \text{and} \quad A_2'(z = +\infty) = \text{const.} \neq 0. \quad (2.16)$$

The requirement that these slopes be asymptotically nonzero removes the $A_1 = A_2 = 0$ solution from our considerations. Eqn. 2.16 allows the constant slopes for A_1 and A_2 to be arbitrary. If they are chosen to be unequal, it implies that the corresponding magnetic fields B_1 and B_2 are unequal, leading to a violation of the symmetry inherent in the problem and this may also cause dynamical instability of the brane as will be discussed further in section 4. Hence, it is natural to choose the slopes to be equal. However, our numerical solutions (see Fig. 3) show that even in the asymmetrical situation, slopes of A_1 and A_2 are very nearly equal.

The coupled differential equations 2.13 and 2.14 together with the conditions of eqns. 2.15 and 2.16 constitute our boundary value problem (BVP).

Since we shall resort to numerics to find solutions it is convenient to transform from coordinate z to u which is defined on a compact interval, $u \in [-1, 1]$, via

$$u = \tanh(v\sqrt{\lambda_1}z). \quad (2.17)$$

With this change of coordinates and the field rescalings

$$R_a \rightarrow vR_a, \quad A_a \rightarrow vA_a, \quad (2.18)$$

the equations become

$$(1-u^2)^2 \frac{d^2 A_1}{du^2} - 2u(1-u^2) \frac{dA_1}{du} = 2\alpha R_1^2 A_1, \quad (2.19)$$

$$(1-u^2)^2 \frac{d^2 R_1}{du^2} - 2u(1-u^2) \frac{dR_1}{du} = \alpha A_1^2 R_1 + 2R_1(R_1^2 + R_2^2 - 1) + \lambda R_1 R_2^2, \quad (2.20)$$

and $1 \leftrightarrow 2$. We have defined $\alpha \equiv e^2/\lambda_1$ and $\lambda \equiv \lambda_2/\lambda_1$. We see that solutions only depend on two independent coupling constants and not three. In the case of the pure Higgs model with $\alpha = 0$ (see Ref. [4]), if one takes symmetric ($R_1 + R_2$) and anti-symmetric ($R_1 - R_2$) linear combinations of the fields, then the differential equations decouple for the special case of $\lambda = 4$ with analytic solutions,

$$R_1 = \frac{1}{2}(1+u), \quad R_2 = \frac{1}{2}(1-u). \quad (2.21)$$

However, this is not the case in our model for $\alpha \neq 0$.

We shall also be interested in the energy of the solutions we find, thus we need the stress-energy for this system

$$T_{\mu\nu} = 2 \frac{\delta \mathcal{L}}{\delta g^{\mu\nu}} - g_{\mu\nu} \mathcal{L}, \quad (2.22)$$

which for our action yields

$$\begin{aligned} T_{\mu\nu} = & -F_{1\mu\alpha} F_{1\nu}^\alpha - F_{2\mu\alpha} F_{2\nu}^\alpha + 2(D_{1\mu}\phi_1)^*(D_{1\nu}\phi_1) + 2(D_{2\mu}\phi_2)^*(D_{2\nu}\phi_2) \\ & + g_{\mu\nu} \left[\frac{1}{4} F_1^{\mu\nu} F_{1\mu\nu} + \frac{1}{4} F_2^{\mu\nu} F_{2\mu\nu} - (D_1^\mu \phi_1)^*(D_{1\mu}\phi_1) - (D_2^\mu \phi_2)^*(D_{2\mu}\phi_2) \right. \\ & \left. + V(\phi_1, \phi_2) \right]. \end{aligned} \quad (2.23)$$

The energy density is then given by the T_{00} component of the stress-energy tensor. This simplifies to

$$\begin{aligned} T_{00} = & \frac{1}{4} \left[(A_1'(z))^2 + (A_2'(z))^2 \right] + (R_1'(z))^2 + (R_2'(z))^2 \\ & + e^2 A_1(z)^2 R_1(z)^2 + e^2 A_2(z)^2 R_2(z)^2 + V(R_1, R_2), \end{aligned} \quad (2.24)$$

for our static solutions and because of our gauge choice, $A_0 = 0$. Thus, in terms of the coordinate u and the rescaled fields the energy density is given by

$$\begin{aligned} \frac{T_{00}}{\lambda_1 v^4} = & (1-u^2)^2 \left[\frac{(\partial_u A_1(u))^2}{4} + \frac{(\partial_u A_2(u))^2}{4} + (\partial_u R_1(u))^2 + (\partial_u R_2(u))^2 \right] \\ & + \alpha A_1(u)^2 R_1(u)^2 + \alpha A_2(u)^2 R_2(u)^2 + (R_1(u)^2 + R_2(u)^2 - 1)^2 \\ & + \lambda R_1(u)^2 R_2(u)^2, \end{aligned} \quad (2.25)$$

where $\lambda_1 v^4$ sets the scale.

3. Numerical Solutions

The numerical method we employ to solve these coupled differential equations is the ‘shooting method’ using the routines from Numerical Recipes in C++ [9]. One can readily convert our system of four coupled second order differential equations to a system of eight coupled first order differential equations where the functions are: $R_1, R_2, A_1, A_2, R'_1, R'_2, A'_1$ and A'_2 . This is a boundary value problem with the functions R_1, R_2, A_1, A_2 are specified on two boundaries but with the functions R'_1, R'_2, A'_1, A'_2 not specified on either boundary. The way the ‘shooting method’ works is that one guesses values for the derivative functions at the left boundary ($u = -1$), then with all the functions specified on the left boundary one can numerically integrate to the right boundary. One then defines a function which measures how well the boundary conditions on the right are matched. Using this goodness of fit function one can then use a Newton-Raphson procedure to improve the guess on the left boundary for the derivatives. One can then iterate this procedure until the boundary conditions on both sides are satisfied to the desired accuracy. One potential difficulty is that if the differential equations are reasonably complicated (e.g. non-linear) then the *initial guess* might need to be reasonably good in order for the procedure to converge.

The differential equations, 2.19 and 2.20, have poles at $u = \pm 1$ when one expresses the equations as $dX/du = (1 - u^2)^{-2} \times \dots$. Since we cannot evaluate these equations at $u = \pm 1$, we set the boundaries at $u_1 = -1 + \epsilon$ and $u_2 = 1 - \epsilon$. However, because now our boundaries are not at $u = \pm 1$ ($z = \pm\infty$) we need to know the asymptotic behavior of our functions in order to set up the boundary conditions correctly². For the special case of $\alpha = 0$ and $\lambda = 4$ the analytic solution, eqn. 2.21, is known from Ref. [4]. While these are not the correct solutions for general α and λ , they do exhibit the correct asymptotic behavior as $u \rightarrow \pm 1$. But as long as ϵ is sufficiently small the correct asymptotic behavior is obtained numerically. When we solve our boundary value problem numerically we shall use eqn. 2.21 to set the boundary conditions for R_1 and R_2 . We also need to know the asymptotic behavior of the gauge fields near the boundaries. Substituting $A = (1 - u^2)^\beta$ into the differential equation for A (eqn. 2.19), we can solve for β , the scaling behavior in the vicinity of the boundary. Thus

$$A_1 \sim (1 - u)\sqrt{\alpha/2} \sim \epsilon\sqrt{\alpha/2} \quad \text{as} \quad u \rightarrow u_2 = 1 - \epsilon \quad (3.1)$$

$$A_2 \sim (1 + u)\sqrt{\alpha/2} \sim \epsilon\sqrt{\alpha/2} \quad \text{as} \quad u \rightarrow u_1 = -1 + \epsilon. \quad (3.2)$$

The values of $A_1(u_1)$ and $A_2(u_2)$ are not constrained by any of the differential equations and are therefore left as free parameters.

As mentioned before when solving a boundary value problem using the ‘shooting method’, convergence may depend on a reasonably accurate guess of the initial conditions on the left boundary. This is the case for our set of differential equations since they have an explicit pole at $u = \pm 1$. This sensitivity gets worse as ϵ approaches zero. The method we employed to address this issue involved starting with a relatively large value of ϵ ($\epsilon = 0.5$) and incrementally

²For numerical reasons we can not just set $R_1(u_1) = 0, R_1(u_2) = 1 \dots$

reducing it to its desired value using as the initial guess for the values of the derivatives (R'_1 , R'_2 , A'_1 and A'_2) on the left boundary for each step the solution of the previous step.

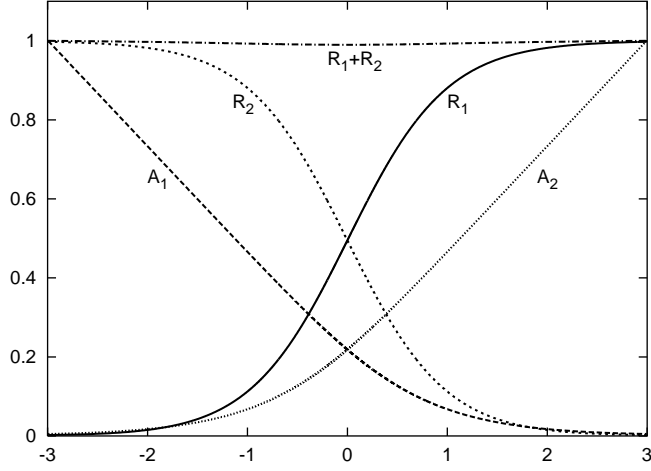


Figure 1: Plot of R_1 , A_1 , R_2 , A_2 and $R_1 + R_2$ against $\tanh^{-1}(u)$ for $\alpha = 1$, $\lambda = 4$. The free boundary conditions are $A_1(-1 + \epsilon) = A_2(1 - \epsilon) = 1$ for $\epsilon = 0.005$ which corresponds to left and right boundaries at $\tanh^{-1}(u) = \pm 3$. $R_1 + R_2$ is nearly constant for this pair of parameters.

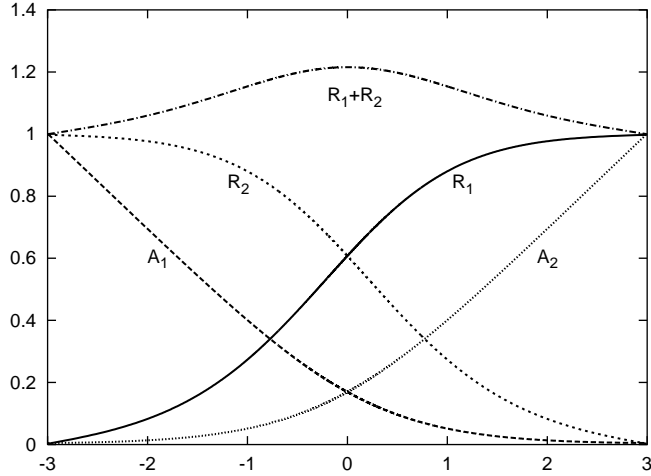


Figure 2: Plot of R_1 , A_1 , R_2 , A_2 and $R_1 + R_2$ against $\tanh^{-1}(u)$ for $\alpha = 1$, $\lambda = 1$. Here $A_1(-1 + \epsilon) = A_2(1 - \epsilon) = 1$ for $\epsilon = 0.005$.

In figs. 1, 2 and 3 we see numerical solutions to these differential equations for a variety of couplings, α , λ and boundary conditions $A_1(u_1)$ and $A_2(u_2)$. We observe that the gauge fields A_1 and A_2 become linear functions of $\tanh^{-1}(u)$ as $u \rightarrow u_1$ and $u \rightarrow u_2$ respectively. This implies that asymptotically these gauge fields become linear functions of z , which corresponds to a constant magnetic field in the direction perpendicular to both z and \tilde{x} (the direction in

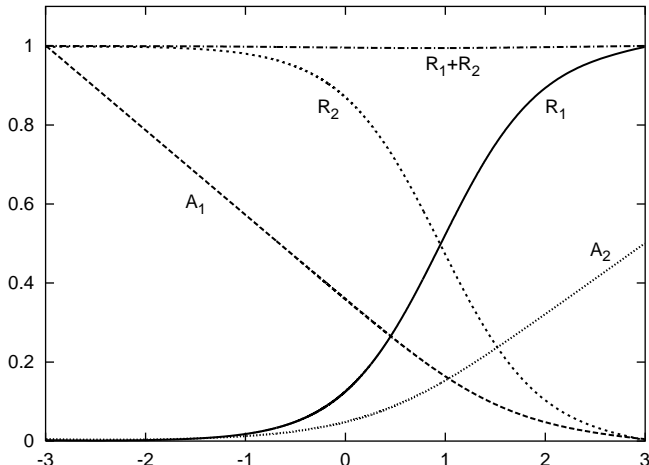


Figure 3: Plot of R_1 , A_1 , R_2 , A_2 and R_1+R_2 against $\tanh^{-1}(u)$ for $\alpha = 1$, $\lambda = 4$. Here $A_1(-1+\epsilon) = 1$ and $A_2(1-\epsilon) = 0.5$ for $\epsilon = 0.005$. The principal effect of the asymmetrical BC's is to shift the center of the brane to the right.

which the gauge field points),

$$B_{\tilde{y}} \sim \partial_z A_{\tilde{x}}(z) = \text{constant}. \quad (3.3)$$

Thus the asymptotic solution (actually $\tanh(u)^{-1}$ need only be of the order of ± 2 to be in the asymptotic regime for a typical configuration) on either side of the domain wall is a constant magnetic field corresponding to the $U(1)$ fields, which point in uncorrelated directions parallel to the domain wall. These solutions have non-zero energy density away from the domain wall and thus are infinite energy configurations. The solutions where the magnetic fields are both zero corresponds to the choice of $\alpha = 0$ (i.e. no $U(1)$ gauge fields).

In figs. 1 and 2, we have set $A_1(u_1 = -0.995) = A_2(u_2 = 0.995) = 1$. With this set of symmetric boundary conditions the domain wall is centered at $u = 0$. In fig. 3 we see that the effect of asymmetric BC's is to shift the location of the domain wall. While not apparent in the figure the magnitudes of the uniform magnetic field far from either side of the domain wall do not exactly match. The choice of $\epsilon = 0.005$ (and $\epsilon = 0.001$ for figs. 5 and 6) corresponds to boundaries at $\tanh(u)^{-1} = \pm 3$ (and ± 3.8). While ϵ can be made smaller at the expense of longer computing time, these values are sufficiently small for our purposes.

In fig. 4 we see the energy density of a solution plotted as a function of the transverse direction. We see that the energy density is peaked at the center of the domain wall. If we treat the asymptotic constant magnetic field on either side of the domain wall as a background, then we can compute the energy per unit surface area of the domain wall by subtracting off the infinite energy associated with the magnetic field. In fig. 5 the surface energy density is plotted as a function of λ for a variety of values of α (boundary conditions are $A_1(-1+\epsilon) = A_2(1-\epsilon) = 1$ at $\epsilon = 0.001$). Observe that this 'renormalized' surface energy density is only weakly dependent on the value of the gauge coupling constant α . In fig. 6 we show the

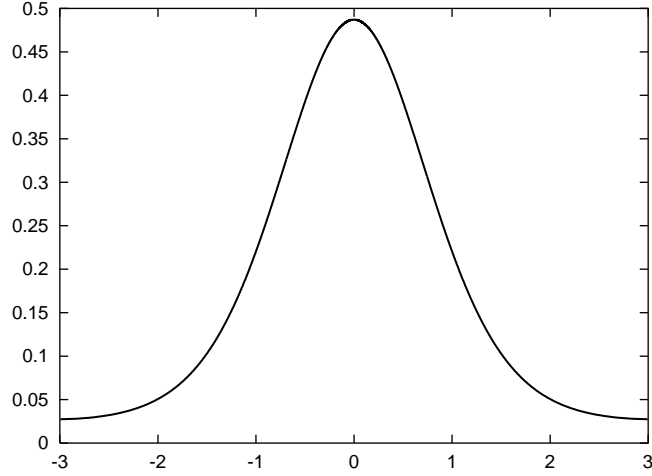


Figure 4: Plot of the energy density against $\tanh^{-1}(u)$ for $\alpha = 1$, $\lambda = 1$. We have used the boundary conditions $A_1(-1 + \epsilon) = A_2(1 - \epsilon) = 1$ where $\epsilon = 0.005$.

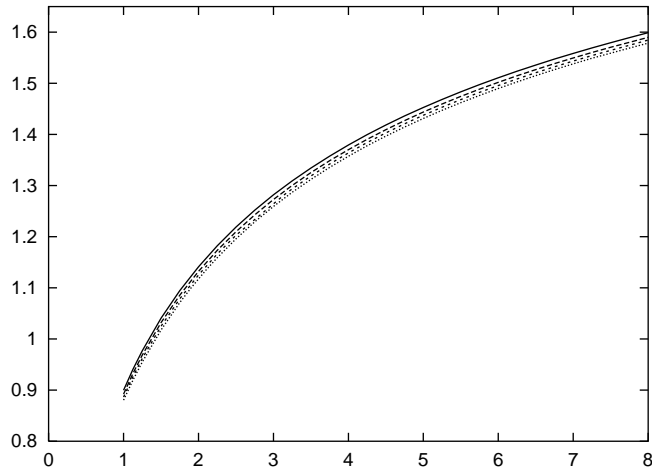


Figure 5: Plot of the ‘renormalized’ surface energy density against λ for $\alpha = 0.25, 0.5, 1.0, 2.0$ (from top to bottom). We have used the boundary conditions $A_1(-1 + \epsilon) = A_2(1 - \epsilon) = 1$ where $\epsilon = 0.001$.

subtracted energy density corresponding to the constant magnetic field as a function of λ and α . In both figs. 5 and 6 we omit values of $\lambda < 1$ as they require a significantly smaller value for ϵ .

Our solutions are all plotted in units of $\tanh(u)^{-1}$ and not z since u is the natural variable in our system of equations, 2.19 and 2.20. The length scale $\tanh(u)^{-1}$ is dimensionless and can be converted into a physical length by dividing by $v\sqrt{\lambda_1}$. The thickness of the domain wall is typically $\sim 4/v\sqrt{\lambda_1}$ (see fig. 4) which can be made arbitrarily small by choosing $v\sqrt{\lambda_1} \gg 1$.

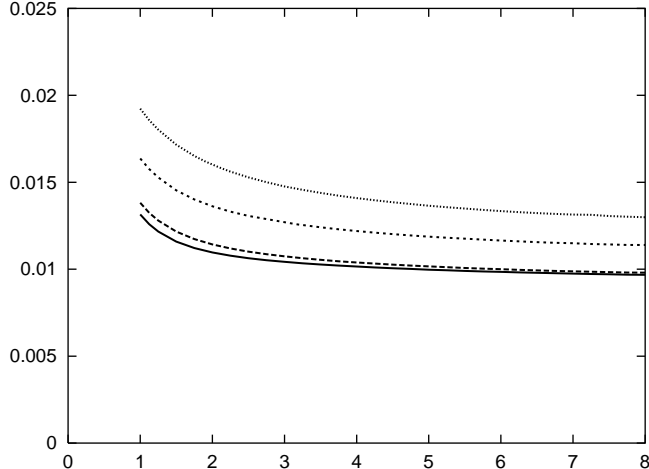


Figure 6: Plot of the energy density of the uniform magnetic field against λ for $\alpha = 0.25, 0.5, 1.0, 2.0$ (from bottom to top). We have used the boundary conditions $A_1(-1 + \epsilon) = A_2(1 - \epsilon) = 1$ where $\epsilon = 0.001$.

4. Discussion

The numerical solutions displayed above have a natural interpretation in terms of superconductivity. Consider, for instance, the currents associated with the $U(1)$ gauge groups,

$$J_{i\mu} = ie[\phi_i^*(\partial_\mu\phi_i) - (\partial_\mu\phi_i^*)\phi_i] + 2e^2 A_{i\mu}\phi_i^*\phi_i, \quad (4.1)$$

where $i = 1, 2$. In terms of the amplitude and phase of ϕ_i , the currents are given by

$$J_{i\mu} = -2eR_i^2\partial_\mu\alpha_i + 2e^2 A_{i\mu}R_i^2. \quad (4.2)$$

For our configurations, which depend only on z , and for which eqn. 2.10 holds, it is clear that only the x - and y -components are non-vanishing. They evaluate to

$$J_{i\,x,y}(z) = 2e^2 A_{i\,x,y}(z)R_i^2(z). \quad (4.3)$$

These steady, z -dependent current densities are uniform supercurrent densities localised to the domain wall, with the charged boson fields as the current carriers.

Equation 4.3 shows that the currents are nonzero only when the gauge field configurations are nonzero and vice-versa, so these currents are responsible for dynamically generating the magnetic fields. On the side of the wall where $R_i \neq 0$, the corresponding magnetic field is seen to decay exponentially, which is simply a Meissner effect. On the other side of the wall, where R_i is tending exponentially quickly to zero, we find the magnetic field \vec{B}_i tending towards a finite, uniform configuration pointing in the plane of the wall. This is consistent with the domain wall carrying a uniform sheet of current density pointing in the $(0, A_{i\,x}, A_{i\,y}, 0)$ direction, as per eqn. 4.3. Our configurations have infinite energy because the domain wall is of infinite extent, with current densities uniformly distributed on it.

The stability or otherwise of our solutions is an important concern. While a complete stability analysis is beyond the scope of this paper, the above considerations suggest that the geometrically symmetric solutions such as in figs. 1 and 2 could be stable, whereas asymmetric configurations such as those of fig. 3 are not. Let current J_1 point in the x -direction in the plane of the wall. Then eqn. 4.3 implies that A_1 also points in the same direction, so \vec{B}_1 is directed along the y -axis. The Lorentz force on the type 1 charge carriers lies in the negative z direction. For sector 2, similar reasoning shows that the corresponding Lorentz force on type 2 charge carriers points in the positive z direction. For symmetric boundary conditions, these forces are equal in magnitude as well as opposite in direction. This is a necessary condition for stability. For asymmetric boundary conditions, they are unequal, strongly suggesting that such configurations are unstable.

5. Conclusions

In order to further explore the idea of the “clash of symmetries” from [4], we have considered a model in which two scalar fields are coupled to their respective gauge fields in a Lagrangian which has $U(1) \times U(1)$ symmetry. We find consistent static solutions for field configurations with the vacuum conditions for the scalar fields specified by eqn. 2.7 and the implied boundary conditions for the gauge fields, eqn. 2.15. We obtain the expected kink-like solutions for the scalar fields while the two gauge fields diverge linearly on either side of the domain wall.

When we consider the idealized configuration of an infinitely thin domain wall, we have solutions such that while the $U(1)$ symmetries of the fields are preserved in their respective vacua, they are both broken on the domain wall. The gauge fields show that the domain wall is sandwiched between domains with constant magnetic fields parallel to the wall. In the case of a domain wall of finite thickness, there will be magnetic fields parallel to the wall on either side. These are associated with superconducting currents, as in the case of the superconducting string solution [1].

This model demonstrates that in addition to the breakdown of symmetries on the brane, the presence of gauge fields introduces new phenomena, such as the appearance of magnetic fields. Background magnetic fields of this kind are reminiscent of the configurations in string theory that give rise to non-commutativity of space-time coordinates. It would be very interesting to see the logical extension of this model to domain wall solutions with non-Abelian gauge fields and to study their dynamical effects in addition to symmetry breaking.

Acknowledgments

This work was supported in part (JSR and KCW) by the U.S Department of Energy (DOE) under contract no. DE-FG02-85ER40237. RRV was supported partially by the Australian Research Council and partially by the University of Melbourne. He thanks his coauthors for their excellent hospitality at Syracuse University where this work was begun.

References

- [1] E. Witten, Nucl. Phys. B **249**, 557 (1985).
- [2] R. MacKenzie, Nucl. Phys. B **303**, 149 (1988).
- [3] Y. Lemperiere and E. P. Shellard, Nucl. Phys. B **649**, 511 (2003) [arXiv:hep-ph/0207199].
- [4] A. Davidson, B. F. Toner, R. R. Volkas and K. C. Wali, Phys. Rev. D **65**, 125013 (2002) [arXiv:hep-th/0202042].
- [5] L. Pogosian and T. Vachaspati, Phys. Rev. D **62**, 123506 (2000) [arXiv:hep-ph/0007045]; see also T. Vachaspati, Phys. Rev. D **63**, 105010 (2001) [arXiv:hep-th/0102047]; L. Pogosian and T. Vachaspati, Phys. Rev. D **64**, 105023 (2001) [arXiv:hep-th/0105128].
- [6] E. Shin and R. R. Volkas, Phys. Rev. D (in press) [arXiv:hep-ph/0309008].
- [7] J. R. Morris, Phys. Rev. D **52**, 1096 (1995).
- [8] G. Lazarides and Q. Shafi, Phys. Lett. B **159**, 261 (1985).
- [9] B. P. Flannery, W. H. Press, S. A. Teukolsky and W. T. Vetterling, “Numerical Recipes in C++,” (second edition), Cambridge University Press, New York, 2002.